New solutions of QCD as models for hadrons and rings of confined gluons

S. M. Mahajan and P. M. Valanju
Department of Physics, University of Texas at Austin, Austin, Texas 78712
(Received 14 May 1987)

Newly found exact, toroidal solutions of QCD are used as confining background chromomagnetic fields to construct confined-gluon rings and hadrons. A semiclassical treatment indicates stable confined-gluon-ring and hadron states with large internal quark motions. Similarities and differences with currently popular bag models are noted.

I. INTRODUCTION

Although it is widely believed that quantum chromodynamics (QCD) is the correct theory to describe strong interactions, it has been impossible to extract its exact low-energy consequences because the theory is inherently nonlinear. The large value of the coupling constant makes perturbation theory useless at these length scales, and one has to resort to building models[1-4] with the hope that they will correctly mimic the actual behavior of the theory.

Recently discovered localized, nonperturbative solutions[5] of pure QCD may help bridge this gap and provide a natural substrate for the construction of strongly interacting objects such as mesons, baryons, and glueballs. These derived solutions could be seen as actual realizations of the hypothetical bags[6-14] which have been extensively used to confine quarks[7] and gluons.[8] The chromomagnetic fields of these solutions have the usual desirable features such as finite energy, localization, and no net color charge. They also have a toroidal spatial structure that can confine color currents in a dynamic equilibrium (unlike the static confinement of the color-electric fields). Most importantly, they are exact consequences of QCD. In this paper we study the quantum fluctuations around these classical solutions, with the idea of eventually deriving a spectrum of hadrons based on these toroidal, static, chromomagnetic solutions of the fermion-free SU(3) gauge theory.

We believe that the toroidal nature of our solutions is a crucial factor needed for confinement. As is well known for the electromagnetic case, confinement of objects with (color) charge can occur only if the (color) current is restricted to lie on a nested set of isobaric surfaces traced out by the confining field.[15] For vector fields in three space dimensions, the topological nature of such surfaces is uniquely specified by a theorem due to Poincaré which states: "In Euclidean three-space, the surfaces traced out by the lines of any vector field that is nonzero and finite everywhere are tori." Since the color (gluon) field is a vector field, only a toroidal geometry can assure its utility as a confining field. Notice that this theorem is true for any vector field, electromagnetic or chromomagnetic, linear or nonlinear. Also, the toroidal nature is essential whether one is confining quarks (mesons and baryons) or gluons (glueballs), because it is dictated entirely by the vector nature of the confining field.

Toroidal bags have been studied earlier[16-18] in the context of glueballs. It was observed[16] that the spherical bag cannot support the confined gluons at two poles and hence collapses to a toroidal shape. However, this important observation never received much support. The difficulty of handling toroidal geometry coupled to the belief that quarks (though not gluons) could be confined in spherical bags may account for this. However, we see that if the confinement is due to the vector color fields of QCD, a toroidal shape is essential. In other words, one can certainly postulate spherical confining models, but one cannot derive them from QCD.

Barring the essential difference that our nonperturbative solutions are derived from pure QCD (and hence are toroidal) and not stipulated in an *ad hoc* fashion, they do resemble conventional bags for all calculational purposes. Because of the toroidal nature of our solutions, we will refer to them as "rings," and the pure glue structures (glueballs) made from them as gluerings. The classical field configuration provides the confining bag pressure. Our program to derive the spectrum of the hadrons will therefore follow very closely the path charted out with great care by the bag-model investigators,[6-14] and we will attempt to make contact with conventional bag models wherever possible. The phenomenology is not expected to be very different except in detail. In fact, when the torus is fat (i.e., its major radius r_0 is nearly equal to its minor radius a), as it turns out to be for the lowest-energy states, our rings become almost spheres (with the troublesome poles punched out).

We begin in Sec. II with a brief review of the static, nonperturbative solutions of Ref. 5, clarifying the geometry, and leading to an analytical expression for the total background field energy $\mathcal{E}_b$. This energy increases linearly with the size r_0 of the ring (see Fig. 1), and can be stabilized only when perturbations with internal angular momentum are added to it. If the perturbations are gluonic in nature, we obtain gluerings whose total energy $\mathcal{E}=\mathcal{E}_b+\mathcal{E}_g$ (where $\mathcal{E}_g$ is the energy of the gluonic perturbation) is minimized with respect to the size parameter to obtain a stable state. This and other characteristics of the gluerings are presented in Sec. III, while Sec. IV deals with the fermionic perturbations which generate mesons and baryons. The masses of the gluerings and hadrons are determined completely up to an unknown scale length ϵ which is the skin width of the minimum-energy torus.

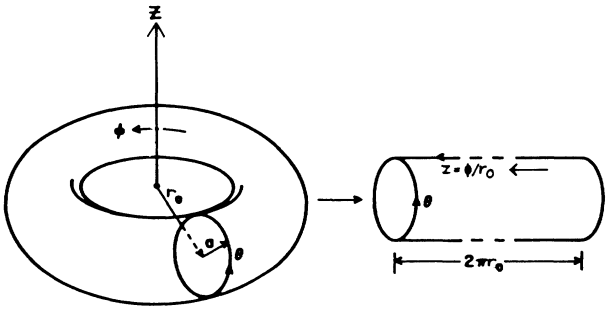

FIG. 1. Mapping of the toroidal geometry to cylindrical geometry.

This undetermined length scale is a consequence of the fact that the underlying theory (QCD) is scale-free. It is likely that the gluerings, mesons, and baryons are characterized by different length scales. Section V ends the paper with a brief summary and discussion of these preliminary results. Detailed spectrum calculations will be provided in a forthcoming paper.

II. CLASSICAL SOLUTIONS

The pure (quark-free) SU(N) Yang-Mills equations are

$$\partial^{\mu}F^{l}_{\mu\nu}+gC^{lmn}A^{\mu m}F^{n}_{\mu\nu}=0 \ , \tag{1}$$

where the color indices l, m, and n go from 1 to 8, the spacetime indices μ and ν go from 0 to 3 (t,r,θ, and ϕ), the field-strength tensor is given by

$$F^{l}_{\mu\nu}=\partial_{\mu}A^{l}_{\nu}-\partial_{\nu}A^{l}_{\mu}+gC^{lmn}A^{m}_{\mu}A^{n}_{\nu} \ , \tag{2}$$

g is the strong coupling constant ($g^2/4\pi\simeq 1$), and C^{lmn} are the structure constants of SU(N). For a static, cylindrically symmetric system ($\partial_t=\partial_\theta=0,\partial_\phi=r_0\partial_z=0$), the ansatz (only A_θ and A_ϕ are nonzero, $A_0=0$ implies no color-electric field)

$$A^{l}_{\mu}=\frac{1}{g}[\eta_l\delta_{\mu 2}P(r)+\zeta_l\delta_{\mu 3}Q(r)] \ , \tag{3}$$

where η_l and ζ_l are two fixed vectors in SU(3), reduces the problem to solving a coupled pair of ordinary differential equations for the functions $P(r)$ and $Q(r)$:

$$\frac{d}{dr}\frac{1}{r}\frac{d}{dr}rP=Q^2P \tag{4a}$$

and

$$\frac{1}{r}\frac{d}{dr}r\frac{dQ}{dr}=P^2Q \ . \tag{4b}$$

Different choices of η_l and ζ_l lead to solutions that can be gauge transformed into each other, but there is no gauge in which either the resulting color-magnetic field totally vanishes or a color-electric field is generated. In Ref. 5, Eqs. (4a) and (4b) are solved exactly for all r, yielding pure chromomagnetic fields that are large only in a toroidal surface region of width ϵ near $r=a$, where a is the minor radius of the torus. The location a and the width ϵ of this large field region are not determined by the theory itself, although stability conditions lead to one relation between them, leaving ϵ as the only undetermined input parameter of the theory, and its value will be determined by fitting the mass spectrum. The existence of one undetermined scale length is a natural consequence of the scale invariance of QCD. We expect that the physics in the surface region will be governed by the production mechanisms for $q\bar{q}$ pairs, leading to a value of ϵ of the order of the universal 200-MeV (1-F) scale.[4] Although the exact mechanism for the generation of ϵ is not clear yet, it is interesting to note that its value will control both the mass spectra as well as the transition rates.

The cylindrical geometry should be viewed as an approximation to the torodial geometry; the leading-order terms are obtained by simulating a torus of major radius r_0 by a cylinder of length $2\pi r_0$, with its ends at $z=0$ and $z=2\pi r_0$ identified with each other (see Fig. 1, the toroidal angle $\phi=r_0^{-1}z$). The z axis of the cylinder will then be the minor axis of the torus, while the major axis will be denoted by Z. Any internal linear momentum p_z along the minor axis z will correspond to the Z component of an internal angular momentum $L_z=r_0p_z$ along the major axis Z. Note that the torus has its principal symmetry about the Z axis, which should not be confused with the approximate cylindrical symmetry around the minor z axis. This approximation is good for a thin torus ($r_0\ll a$), but corrections have to be added for a fat torus ($r_0\simeq a$). The geometry also imposes a physical constraint on the lengths

$$\epsilon<a<r_0 \ . \tag{5}$$

The total energy of the field is the gauge-invariant quantity[5]

$$\mathcal{E}_b=\frac{\pi}{2g^2}r_0\left[\frac{\alpha a}{\epsilon^3}+\frac{\beta}{a^2}\right] , \tag{6}$$

where α and β are numerical constants which depend on the gauge group and the choice of the SU(3) vectors η_l and ζ_l. For a typical case discussed in Ref. 5, $\alpha=1.7$ and $\beta=12$. The classical energy increases linearly with r_0, and is not stable to an overall shrinking of the solution. The fields thus exert an inward pressure which has to be balanced by an outward pressure coming from any fluctuations confined within this ring. We shall see that the rotation of the constituents around the Z axis will provide the appropriate centrifugal force required to achieve an equilibrium configuration.

Although the "ring" has strong color-magnetic fields near the surface, its net color charge is zero (there are no long-range color-electric or -magnetic fields)—the magnetic field is self-generated by the effective color currents arising from the nonlinearity. This strong surface field can confine any color charge current within the ring, including that of gluons since they too carry color charge. Maintaining net color charge neutrality requires that the stabilizing fluctuations (gluons or quarks) must be in the singlet state because the introduction of any nonsinglets in the ring will give rise to deconfining color-electric fields along which color charges can accelerate and escape.

In the next section, we study pure gluons confined in

our ring. The exact calculation needs to be done fully nonlinearly—an almost impossible task. However, in finding the classical solutions, we have already done much of the work. We can now consider the time-varying fields as perturbations and expand around our classical solutions to obtain a good approximation to the spectrum of low-energy states. Neither the classical solution, nor the spectrum of states built on it can be reached via perturbation theory around the free vacuum. This is evident from the appearance of $1/g^2$ in the expression for the energy. A nonperturbative solution as this one cannot be thought of as a bound state of any finite number of perturbative "gluons."

III. GLUERINGS

We now consider small perturbations in the gluon field around the static equilibrium configuration

$$F^l_{\mu\nu}=F^{l0}_{\mu\nu}+f^l_{\mu\nu} \tag{7}$$

and

$$A^l_\mu=A^{l0}_\mu+a^l_\mu \ , \tag{8}$$

where the static classical solution is denoted by a superscript 0 and the time-dependent perturbing fields a^l_μ and $f^l_{\mu\nu}$ are small. Introducing (7) and (8) into the field equation (1), and linearizing the system leads to a set of complicated coupled differential equations which can only be solved numerically. Several analytical approximations are possible, e.g., in Ref. 5 the short-wavelength limit ($\lambda \ll a$) was investigated, and it was shown that the high-energy gluons acquired a mass due to the background field. In this paper, however, we are interested in calculating the low-energy mass spectrum, so we must deal with fluctuations with wavelengths comparable to the size of the ring. We can do this by making a set of physically motivated assumptions.

The very large color-magnetic field near the surface of the ring confines any color current, including the gluons that carry color charge. Except near the surface, the color field is small. Therefore, we can approximate the effect of the ring by studying free gluon fields confined within a toroidal region by suitable boundary conditions imposed at the surface. The additional effects of the finite skin width can later be added as perturbations. Such a toroidal glueball has been considered earlier by Robson,[16] and we will proceed along similar lines, although with one important difference. He solved the equations in a cylinder around the major axis of the torus, necessitating an unphysical rectangular cross section. The exclusion of the center region also led to a spurious TEM mode. Instead, we make use of the approximate cylindrical symmetry (to order a/r_0) around the minor (z) axis of the torus.

Inside the ring we assume the gluon field to be free, i.e., each color gluon component separately obeys the free Maxwell's equations

$$\nabla^2\overline{\mathbf{E}}=\frac{\partial^2\overline{\mathbf{E}}}{\partial t^2} \tag{9}$$

and

$$\nabla^2\overline{\mathbf{B}}=\frac{\partial^2\overline{\mathbf{B}}}{\partial t^2} \ . \tag{10}$$

At this point, we neglect the gluon-gluon interaction; it will be included as a perturbation in later work. Since our equilibrium solutions depend only on r (in this case, just a set of boundary conditions at $r=a$), we expand the perturbed quantities in poloidal and toroidal harmonics (where θ is the poloidal and $\phi=z/r_0$ is the toroidal angle, and both θ and ϕ are symmetry directions):

$$\begin{aligned}\overline{\mathbf{E}}&=\mathbf{E}(r)e^{-i\omega t+im\theta+il\phi} \ ,\\ \overline{\mathbf{B}}&=\mathbf{B}(r)e^{-i\omega t+im\theta+il\phi} \ ,\end{aligned} \tag{11}$$

where ω is the frequency and m and l are the poloidal and toroidal quantum numbers. The z components of both $\mathbf{E}$ and $\mathbf{B}$ satisfy the same radial equation

$$\left[\frac{1}{r}\frac{d}{dr}r\frac{d}{dr}-\frac{m^2}{r^2}+\mu^2\right]E_z(r)=0 \ , \tag{12}$$

where

$$\mu^2=\omega_{lmn}{}^2-\frac{l^2}{r_0{}^2} \ , \tag{13}$$

serves as the effective eigenvalue. Note that we have suppressed the color indices totally because each color component satisfies the same equation. Equation (12) is easily solved to obtain the radial dependence of the z components of E and B:

$$E_z(r)=E_0J_m(\mu r) \tag{14}$$

and

$$B_z(r)=B_0J_m(\mu r) \ , \tag{15}$$

where $J_m(\mu r)$ are ordinary Bessel functions. Note that the Neumann functions have been rejected by demanding that the solutions be finite at the origin. All other field components can be calculated from E_z and B_z by using

$$\nabla\times\mathbf{E}=\frac{i\omega}{c}\mathbf{B} \tag{16}$$

and

$$\nabla\times\mathbf{B}=-\frac{i\omega}{c}\mathbf{E} \ , \tag{17}$$

to give

$$E_r=\frac{1}{\mu^2}\left[ik_z\frac{\partial E_z}{\partial r}-\frac{m\omega}{r}B_z\right] \ , \tag{18}$$

$$E_\theta=\frac{1}{\mu^2}\left[i\omega\frac{\partial B_z}{\partial r}+\frac{k_zm}{r}E_z\right] \ , \tag{19}$$

$$B_r=\frac{1}{\mu^2}\left[ik_z\frac{\partial E_z}{\partial r}+\frac{m\omega}{r}E_z\right] \ , \tag{20}$$

$$B_\theta=-\frac{1}{\mu^2}\left[-i\omega\frac{\partial E_z}{\partial r}+\frac{k_zm}{r}B_z\right] \ , \tag{21}$$

where $k_z=l/r_0$ is the momentum in the toroidal direction

so that l becomes the internal angular momentum along the major axis (Z) of the torus. The boundary conditions at $r=a$ are[2]

$$\hat{\mathbf{n}}\cdot\mathbf{E}=0\ ,\qquad \hat{\mathbf{n}}\times\mathbf{B}=0\ , \tag{22}$$

where $\hat{\mathbf{n}}$ is the outward unit normal to the ring surface.

Just as in the electromagnetic waveguide, the eigenmodes separate into transverse (chromo)electric (TE, $E_z=0$ everywhere) and transverse (chromo)magnetic (TM, $B_z=0$ everywhere) modes. The TEM mode is not allowed by the boundary condition at the origin. For the TE mode, the boundary conditions (22) are satisfied if

$$J_m(\mu a)=0\ , \tag{23}$$

leading to the dispersion relation

$$\omega_{lmn}{}^2-\frac{l^2}{r_0{}^2}=\frac{\alpha_{mn}{}^2}{a^2}\ , \tag{24}$$

where α_{mn} is the nth zero of the mth Bessel function. Similarly, for the TM mode, the boundary condition

$$J_m'(\mu a)=0 \tag{25}$$

leads to the dispersion relation

$$\omega_{lmn}{}^2-\frac{l^2}{r_0{}^2}=\frac{\beta_{mn}{}^2}{a^2}\ , \tag{26}$$

where β_{mn} is the nth zero of the derivative of the mth Bessel function. If we denote both α_{mn} and β_{mn} by the generic symbol $\lambda_{m,n}=\lambda_{-m,n}$, the total energy of the perturbation is given by

$$\mathcal{E}_{lmn}=\hbar\omega_{lmn}=\hbar\left[\frac{l^2}{r_0{}^2}+\frac{\lambda_{mn}{}^2}{a^2}\right]^{1/2}\ . \tag{27}$$

Notice that the $m=0$ TM mode has the same dispersion relation as the $m=1$ TE mode. The lowest mode is the $m=1$ TM mode with

$$\omega_{l,1,1}{}^2=\frac{l^2}{r_0{}^2}+\frac{(1.841)^2}{a^2}\ , \tag{28}$$

followed by the $m=0$ TE mode with

$$\omega_{l,0,1}{}^2=\frac{l^2}{r_0{}^2}+\frac{(2.405)^2}{a^2}\ . \tag{29}$$

The energy of the fluctuations has to be added to the background ring energy to obtain the total energy of the gluering. However, any arbitrary addition of fluctuations will not lead to physically meaningful objects—the final state must be colorless. Since the net color charge of the background ring is zero in any gauge, only color-singlet combinations of gluons can lead to observable states. The lowest-energy gluering will, naturally, have two gluons. The total energy of a gluering state with N gluons is given by a sum of the ring and gluon energies:

$$\mathcal{E}_{\rm tot}^{L}=\mathcal{E}_b+\sum_{i=1}^{N}\left[\frac{l_i{}^2}{r_0{}^2}+\frac{\lambda_{mni}{}^2}{a^2}\right]^{1/2}\ , \tag{30}$$

where the Z component of the total internal angular momentum is given by

$$L_Z=\sum_{i=1}^{N} l_i\ . \tag{31}$$

The total spin S of the gluons has to be added to L to obtain the total spin J of the gluering.[19] A nonspherical object such as the gluering must be treated like a distorted nucleus,[20] giving rise to a tower of rotating states based on each internal L_Z. These states correspond to an addition of the internal and the body angular momenta, and are constructed by a suitable Clebsch-Gordan combination. We will restrict our attention to the lowest state (corresponding to zero angular momentum for the rotation of the body axis). In that case, the total orbital angular momentum is equal to the internal orbital angular momentum ($L=L_Z$), the spin is S, and the total angular momentum is $J=L+S$. The parity is $(-1)^L$ for the TM modes and $-(-1)^L$ for the TE modes.

The stable N-gluon state is obtained by minimizing the total energy as a function of a and r_0 (while holding the input parameter ϵ constant) to obtain the simultaneous equations

$$\left.\frac{\partial\mathcal{E}}{\partial a}\right|_{a=a_0,r=\bar{r}_0}=\frac{\pi\bar{r}_0}{2g^2}\left[\frac{\alpha}{\epsilon^3}-\frac{2\beta}{a_0{}^3}\right]-\sum_{i=1}^{N}\frac{\lambda_{mni}{}^2}{a_0{}^3}\left[\frac{l_i{}^2}{\bar{r}_0{}^2}+\frac{\lambda_{mni}{}^2}{a_0{}^2}\right]^{-1/2}=0 \tag{32}$$

and

$$\left.\frac{\partial\mathcal{E}}{\partial\bar{r}_0}\right|_{a=a_0,r=\bar{r}_0}=\frac{\pi}{2g^2}\left[\frac{\alpha a_0}{\epsilon^3}+\frac{\beta}{a_0{}^2}\right]-\sum_{i=1}^{N}\frac{l_i{}^2}{\bar{r}_0{}^3}\left[\frac{l_i{}^2}{\bar{r}_0{}^2}+\frac{\lambda_{mni}{}^2}{a_0{}^2}\right]^{-1/2}=0\ , \tag{33}$$

which must be solved to obtain the optimum minor (a_0) and major ($\bar{r}_0$) radii. For $\alpha=1.7$, $\beta=12$, and any given values of g and λ_{mni}, the geometrical constraint $\bar{r}_0\geq a_0$ puts restrictions on the values of $|l_i|$. For the special case of the two-gluon ring with $|l_1|=|l_2|=|l|$, this restriction requires that $|l|$ must exceed a critical value l_c; i.e., the internal gluon angular momentum (about the major Z axis) must be large enough for the centrifugal force to prevent the collapse of the major radius. The two gluons in the lowest-energy stable state are in $n_1=n_2=1$, $|m_1|=|m_2|=1$ TM modes ($\lambda_{mn}=\lambda_{11}=1.84$). This state is stable for $|l|\geq l_c=4$ for $g^2/4\pi=1$. The exact value of the lower limit l_c is somewhat sensitive to the strength of g. For a larger value of g, the background energy and hence the minimum value of l required for stabilization is decreased. Also, if the number of gluons is increased, each one of them can be in a lower l state, but the total state will have a higher energy. It is clear that the total energy of the minimum configuration obtained

by the above procedure is inversely proportional to the only length parameter in the theory, i.e., ϵ. Since $\bar{r}_0$ gets related to ϵ in the minimization procedure, it turns out to be more convenient to express the minimum energy as

$$\mathcal{E}_{\min}=\frac{\Delta}{\bar{r}_0} , \tag{34}$$

where $\Delta=3.15$ (F GeV) for the above case (with $\mathcal{E}$ in GeV and $\bar{r}_0$ in F). The energy is inversely proportional to ϵ. For a state with two gluons having opposite angular momenta, with $\epsilon=1$ fm and $g^2/4\pi=1$, we find the total energy $\mathcal{E}=1.05$ GeV, the energy in the background ring $\mathcal{E}_b=0.47$ GeV, the major radius $\bar{r}_0=3.0$ F, and the minor radius $a_0=2.7$ F. The lowest state thus obtained has two gluons in $l_i=\pm 4$ giving total $L=0$, and $J^{PC}=0^{++}$ or 2^{++}. If we wish to identify this gluering with the $\iota(1440)$ (Ref. 21), we need an $\epsilon=0.73$ F, which is quite a reasonable value. Unlike earlier bag models, however, our theory demands that the constituent gluons must have high internal angular momenta even when the total angular momentum of the ring is zero. Since the internal angular momentum stabilizes the linear increase in the background ring energy, this is an essential prediction of our model.

The next excited states arise from $l_1=5$ and $l_2=-4$, with $L=1$, and are at a higher energy. Some of these states are spurious in the sense described in Ref. 17. The details of the resulting gluering spectrum and possible identifications of the predicted states are currently under investigation.

IV. THE HADRON SECTOR

To construct hadrons we have to insert quarks instead of gluons in the ring. The large chromomagnetic field at the edge confines quarks, while inside the ring they are almost free. We could therefore employ an approximation similar to Sec. III, solving for free quarks with confining boundary conditions at the edge. However, we do not need to make this approximation, because the Dirac equation in the desired color field of the ring can, in fact, be solved. The resulting equation exhibits some striking symmetries which are due to the structure of the background field, and leads to exact solutions for some cases.

Although the background ring field has two components (in the θ and ϕ directions), it is easier to demonstrate the essential features of the calculation by choosing only one component to be nonzero:

$$A_\theta=\frac{P(r)}{g} , \tag{35}$$

where $P(r)$ given in Ref. 5 can be approximated for all r by

$$P(r)=\frac{\sqrt{2}r}{a-r} . \tag{36}$$

The Dirac Hamiltonian in this potential is given by

$$\begin{aligned} H&=\boldsymbol{\alpha}\cdot(\mathbf{p}-g\,\mathbf{A})+\beta m \\ &=\alpha_z p_z-\alpha_\theta\left[\frac{i}{r}\frac{\partial}{\partial\theta}+P\right]-i\alpha_r\frac{\partial}{\partial r} . \end{aligned} \tag{37}$$

In cylindrical geometry, the operators

$$p_z=-i\frac{\partial}{\partial z}\equiv-\frac{i}{r_0}\frac{\partial}{\partial\phi} \tag{38}$$

and

$$k=-i\frac{\partial}{\partial\theta}+\frac{1}{2}\sigma_z' \tag{39}$$

commute with each other and with the Hamiltonian, so that we may construct simultaneous eigenfunctions of H, p_z, and k.

In the Appendix we show how to reduce this problem to a Schrödinger-type equation

$$\left[\frac{d^2}{dx^2}+\mu^2-V(x)\right]\mathcal{R}=0 , \tag{40}$$

where $x=r/a$ is the normalized radial variable and the potential $V(x)$ is given by

$$\begin{aligned} V^{\mp}(x)=&\frac{(k\mp\frac{1}{2})^2-\frac{1}{4}}{x^2}+\frac{2\mp\sqrt{2}}{(1-x)^2} \\ &-\frac{2\sqrt{2}k}{1-x}-\frac{2(1+x)}{1-x} , \end{aligned} \tag{41}$$

with

$$\mu^2=a^2\left[\mathcal{E}^2-m^2-\frac{l^2}{r_0{}^2}\right] , \tag{42}$$

where l takes integral and k takes half-integral values. The upper (lower) sign of $V^{\mp}$ corresponds to the positive- (negative-) helicity state of the quark. Note that k is related to the local z axis (the minor axis of the torus), and not the body Z axis (the major axis of the torus).

Equation (40) is readily solved on a computer with the boundary conditions that the solution be finite both at the origin ($x=0$) and at the surface of the torus ($x=1$) to yield the eigenspectrum

$$\mu_{mn}{}^2=a^2\left[\mathcal{E}_{lmn}{}^2-m^2-\frac{l^2}{r_0{}^2}\right] , \tag{43}$$

where n is the radial mode number of the solution. A list of eigenvalues is given in Table I, and a few representative eigenfunctions are displayed in Fig. 2. For positive values of k, the above equation with the potential $V^-(x)$ has an exact well-behaved solution

$$\psi=e^{\sqrt{2}x}x^k(1-x)^2 , \tag{44}$$

with the eigenvalue $\mu^2=0$. Note that each of these wave functions has exactly one maximum that moves closer to the edge of the torus for higher values of k. This degeneracy will be lifted when toroidal effects are taken into account, yet the $k=\frac{1}{2}$ will still be the lowest mode. Comparing with other values in Table I, it is clear that the

TABLE I. Eigenvalues (μ^2) of Eq. (41).

k	Negative sign in Eq. (42) $n=0$	$n=1$	Positive sign in Eq. (41) $n=0$	$n=1$
$-\frac{7}{2}$	90.82	160.36	90.82	160.36
$-\frac{5}{2}$	61.48	120.65	61.48	120.65
$-\frac{3}{2}$	36.20	84.76	36.20	84.76
$-\frac{1}{2}$	15.43	52.88	15.43	52.88
$\frac{1}{2}$	0.0	25.19	25.19	71.59
$\frac{3}{2}$	0.0	36.05	36.05	92.06
$\frac{5}{2}$	0.0	48.18	48.18	114.29
$\frac{7}{2}$	0.0	61.62	61.62	138.30

combination of positive k and $V^-(x)$ lead to the lowest-energy solutions with $\mu^2=0$.

Having solved the Dirac equation to find the orbitals, we can introduce quark-antiquark pairs or three quarks (in color-singlet states) into them and construct mesons and baryons. For a state with N quarks in angular momenta l_i, the total energy is given by an equation similar to (30):

$$\mathcal{E}_{\rm tot}^{L}=\mathcal{E}_b+\sum_{i=1}^{N}\left[m_i^2+\frac{l_i^2}{r_0^2}+\frac{\mu_i^2}{a^2}\right]^{1/2}, \tag{45}$$

where m_i is the mass of the ith quark, l_i is its internal angular momentum, and μ_i is the eigenvalue of Eq. (40) for that orbital. Again the total angular momentum J is given by $L+S$, where L is total internal angular momentum given by Eq. (31). The charge conjugation is $C=(-1)^{L+S}$, and parity is $P=(-1)^{L+1}$. For given values of ϵ and g, this energy has to be minimized to obtain $\mathcal{E}_{\rm min}, \bar{r}_0$, and a_0. Using the parameters given in the preceding section, we find that for a $q\bar{q}$ system with the quarks set in the opposite l states, a minimum value

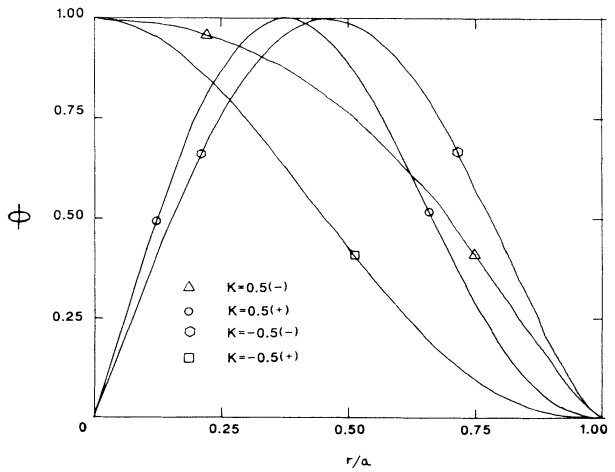

FIG. 2. Eigenfunctions $\phi=x^{-1/2}\mathcal{R}$ of Eq. (41) for four cases: $k=\frac{1}{2}$ and $-\frac{1}{2}$ for the positive and the negative sign in Eq. (40). The eigenvalues are given in Table I.

($|l|=3$) of internal angular momentum is needed to achieve stabilization consistent with the constraint $a_0<\bar{r}_0$. The high internal angular momentum for the quarks is also a new prediction of our model.

If we set q and $\bar{q}$ in ($L=0$, $l_i=\pm 3$) states with their spins opposite to each other, we get the 0^- mesons. For baryons, we can set the three quarks in ($L=0$, $l_i=1,2$, and 3) states to obtain the spin-$\frac{1}{2}$ and spin-$\frac{3}{2}$ baryons depending on their spin alignments. Since we have not yet included the spin-spin interactions of the quarks, the $N^{1/2}$ and $\Delta^{3/2}$ will turn out to be degenerate. It is interesting to note that, after minimization, half of the total energy is in the background ring ($\mathcal{E}_b$), and the other half is carried by all the "valence" quarks together. This seems to agree with the current observations, if we could identify the ring with the "sea." These details of the mass spectrum including the spin-spin interaction will be presented in a forthcoming paper.

V. SUMMARY AND CONCLUSIONS

Using recently found nonperturbative, spatially localized, classical solutions of pure QCD as a confining background, we can construct physically observable, strongly interacting objects: the gluerings and the hadrons. Constraints implied by Poincaré's theorem impose a toroidal geometry on the confining vector color field leading to the first major prediction of our theory: the gluerings and hadrons are tori and not spheres. The stability requirements of these systems lead to the second major prediction: the constituent fluctuations (which are gluons for the gluerings and quarks for the hadrons) must be characterized by higher internal angular momenta about the major axis of the torus. A unified picture of hadrons and gluerings emerges, where both are toroidal states of dynamic equilibrium created by nonlinear QCD fields with and without quarks. Further consequences of the theory including calculation of the detailed mass spectrum (incorporating spin-spin effects) are under investigation.

ACKNOWLEDGMENTS

We would like to thank Dr. J. Sedlak for providing numerical solutions of the fermion eigenvalue equations and the plots of Fig. 2. Discussions with Professor A. Qadir, Professor E. C. G. Sudarshan, and Professor D. Dicus are also acknowledged.

APPENDIX

In the chromomagnetic field given by

$$A_\theta=\frac{P(r)}{g}, \tag{A1}$$

the Dirac Hamiltonian is

$$H=\boldsymbol{\alpha}\cdot(\mathbf{p}-g\,\mathbf{A})+\beta m$$
$$=\alpha_z p_z-\alpha_\theta\left[\frac{i}{r}\frac{\partial}{\partial\theta}+P\right]-i\alpha_r\frac{\partial}{\partial r}. \tag{A2}$$

In cylindrical geometry, the operators

$$p_z = -i\frac{\partial}{\partial z} \equiv \frac{l}{r_0} \tag{A3}$$

and

$$k = -i\frac{\partial}{\partial\theta} + \frac{1}{2}\sigma_z' \tag{A4}$$

commute with each other and the Hamiltonian, so that we can write

$$H = \alpha_z p_z + \alpha_\theta \left[\frac{k}{r} - P - \frac{1}{2}\frac{\sigma_z'}{r}\right] - i\alpha_r \frac{\partial}{\partial r}$$

$$= \alpha_z p_z + \alpha_\theta \left[\frac{k}{r} - P\right] - i\alpha_r \left[\frac{\partial}{\partial r} + \frac{1}{2r}\right] \tag{A5}$$

and look for simultaneous eigenfunctions of H, p_z, and k.

If we write the wave function ψ as $\psi = \begin{pmatrix}\phi\\ \chi\end{pmatrix}$, where ϕ and χ are two-component spinors, and note that $\alpha_\theta \cdot \sigma_z' = i\alpha_r$, the Dirac equation becomes

$$(E-m)\phi = \left[\sigma_z p_z + \sigma_\theta\left[\frac{k}{r} - P\right] - i\sigma_r\left[\frac{d}{dr} + \frac{1}{2r}\right]\right]\chi ,$$

$$(E+m)\chi = \left[\sigma_z p_z + \sigma_\theta\left[\frac{k}{r} - P\right] - i\sigma_r\left[\frac{d}{dr} + \frac{1}{2r}\right]\right]\phi . \tag{A6}$$

Since we are constructing simultaneous eigenfunctions of H and k, we also have

$$\left[-i\frac{\partial}{\partial\theta} + \frac{1}{2}\sigma_z'\right]\psi = k\psi , \tag{A7}$$

where k is now the eigenvalue of the operator in (A4). Equation (A7) is solved to obtain

$$\psi = \begin{bmatrix} \phi_1(r)e^{i(k-1/2)\theta} \\ \phi_2(r)e^{i(k+1/2)\theta} \\ \chi_1(r)e^{i(k-1/2)\theta} \\ \chi_2(r)e^{i(k+1/2)\theta} \end{bmatrix} , \tag{A8}$$

which, when substituted into Eq. (A9) yields the radial equation

$$\left[\frac{d^2}{dr^2} + \frac{1}{r}\frac{d}{dr} + 2\frac{Pk}{r} + \mu^2 - P^2 \pm \frac{dP}{dr} - \frac{(k\mp\frac{1}{2})^2}{r^2}\right]\phi_{1,2} = 0 , \tag{A9}$$

where ϕ_1 obeys (A9) with the upper sign, ϕ_2 with the lower sign, and $\mu^2 = \mathcal{E}^2 - p_z{}^2 - m^2$. Remembering that

$$\sigma_r = \sigma_x\cos\theta + \sigma_y\sin\theta \tag{A10}$$

and

$$\sigma_\theta = -\sigma_x\sin\theta + \sigma_y\cos\theta , \tag{A11}$$

$\chi_{1,2}$ can be calculated from $\phi_{1,2}$ by

$$(E+m)\chi_1(r) = p_z\phi_1(r) - i\left[\frac{d}{dr} - P + \frac{k+\frac{1}{2}}{r}\right]\phi_2(r) ,$$

$$(E+m)\chi_2(r) = -p_z\phi_2(r) - i\left[\frac{d}{dr} - P - \frac{k-\frac{1}{2}}{r}\right]\phi_1(r) . \tag{A12}$$

Two independent sets of positive-energy solutions are obtained by choosing either $\phi_2(r)=0$ or $\phi_1(r)=0$:

$$\psi = \begin{bmatrix} \phi_1(r) \\ 0 \\ \dfrac{p_z}{\mathcal{E}+m}\phi_1(r) \\ -\dfrac{i}{\mathcal{E}+m}\left[\dfrac{d}{dr} - P - \dfrac{k-\frac{1}{2}}{r}\right]\phi_1(r) \end{bmatrix} \quad \text{or} \quad \begin{bmatrix} 0 \\ \phi_2(r) \\ -\dfrac{i}{\mathcal{E}+m}\left[\dfrac{d}{dr} - P + \dfrac{k+\frac{1}{2}}{r}\right]\phi_2(r) \\ -\dfrac{p_z}{\mathcal{E}+m}\phi_2(r) \end{bmatrix} . \tag{A13}$$

We write the eigenvalue equation as

$$\left[\frac{d^2}{dr^2} + \frac{1}{r}\frac{d}{dr} - \frac{(k\mp\frac{1}{2})^2 - \frac{1}{4}}{r^2} + \frac{2k}{r}P + \mu^2 - \left[P^2 \mp \frac{dP}{dr}\right]\right]\phi_{1,2} = 0 . \tag{A14}$$

It is useful to convert the above equation to a one-dimensional Schrödinger-type equation by setting

$$\phi = r^{-1/2}\mathcal{R} , \tag{A15}$$

yielding

$$\left[\frac{d^2}{dr^2} + \frac{(k-\frac{1}{2})^2 - \frac{1}{4}}{r^2} + \frac{2k}{r}P + \mu^2 - \left[P^2 - \frac{dP}{dr}\right]\right]\mathcal{R}_1 = 0 \tag{A16}$$

and

$$\left[\frac{d^2}{dr^2} + \frac{(k+\frac{1}{2})^2 - \frac{1}{4}}{r^2} + \frac{2k}{r}P + \mu^2 - \left[P^2 + \frac{dP}{dr}\right]\right]\mathcal{R}_2 = 0 . \tag{A17}$$

It is clear that the short-distance ($r \to 0$) behavior is dom-

inated by terms proportional to $1/r$ and $1/r^2$, and the behavior for $r \to a$ is controlled by terms containing P. Using the explicit form for P given in Eq. (36) and defining the normalized distance $x = r/a$, Eqs. (A16) and (A17) can be jointly expressed in the Schrödinger-type form

$$\left[\frac{d^2}{dx^2} + \mu^2 - V^{\mp}(x)\right] \mathcal{R}_{1,2} = 0 , \tag{A18}$$

where $x = r/a$ is the normalized radial variable and the potential $V^{\mp}(x)$ is given by

$$V^{\mp}(x) = \frac{(k \mp \frac{1}{2})^2 - \frac{1}{4}}{x^2} + \frac{2 \mp \sqrt{2}}{(1-x)^2} - \frac{2\sqrt{2}k}{1-x} - \frac{2(1+x)}{1-x} \tag{A19}$$

and

$$\mu^2 = a^2 \left[\mathcal{E}^2 - m^2 - \frac{l^2}{r_0^2}\right] . \tag{A20}$$

Notice that l takes integral and k takes half-integral values.

[1]For a review of the various models, see C. Quigg, in *Gauge Theories in High Energy Physics,* edited by M. K. Gaillard and R. Stora (North-Holland, Amsterdam, 1983).

[2]For a review of bag models, see C. E. DeTar and J. F. Donoghue, Annu. Rev. Nucl. Sci. **33**, 235 (1983).

[3]P. Hasenfratz and J. Kuti, Phys. Rep. **40C**, 75 (1978).

[4]J. D. Bjorken, in *Quantum Chromodynamics,* proceedings of the 7th SLAC Summer Institute on Particle Physics, edited by A. Mosher (SLAC, Stanford, 1979), p. 219.

[5]S. Mahajan and P. Valanju, Phys. Rev. D **35**, 2543 (1987).

[6]A. Chodos, R. L. Jaffe, K. Johnson, C. B. Thorn, and V. F. Weisskopf, Phys. Rev. D **9**, 3471 (1974).

[7]T. DeGrand, R. L. Jaffe, K. Johnson, and J. Kiskis, Phys. Rev. D **12**, 2060 (1975).

[8]R. L. Jaffe and K. Johnson, Phys. Lett. **60B**, 201 (1976).

[9]E. Golowich, Phys. Rev. D **12**, 2108 (1975).

[10]E. Golowich, Phys. Rev. D **18**, 927 (1978).

[11]T. Barnes, Nucl. Phys. **B96**, 353 (1975).

[12]T. Barnes, Nucl. Phys. **B152**, 171 (1979).

[13]T. Barnes, F. E. Close, and S. Monaghan, Nucl. Phys. **B198**, 380 (1982).

[14]C. E. Carlson, T. H. Hansson, and C. Peterson, Phys. Rev. D **27**, 2167 (1983).

[15]M. Kruskal, *Plasma Physics* (IAEA, Vienna, 1965), pp. 115–136.

[16]D. Robson, Z. Phys. C **3**, 199 (1980).

[17]J. F. Donoghue, K. Johnson, and B. A. Li, Phys. Lett. **99B**, 416 (1981).

[18]A closed-ring-shaped glue state is indicated in the lattice gauge calculations, for example, J. Kogut, D. Sinclair, and L. Susskind, Nucl. Phys. **B114**, 199 (1976).

[19]C. N. Yang, Phys. Rev. **77**, 242 (1950).

[20]A. de Shalit and H. Feshbach, *Theoretical Nuclear Physics* (Wiley, New York, 1974), Vol. 1, Chap. 6.

[21]P. Roy and T. F. Walsh, Phys. Lett. **78B**, 62 (1978).